2019

Förster resonance energy transfer (FRET) as an optical readout for transcription factor-DNA binding in biosensing applications

BOSTON UNIVERSITY

COLLEGE OF ENGINEERING

Thesis

FÖRSTER RESONANCE ENERGY TRANSFER (FRET)

AS AN OPTICAL READOUT FOR TRANSCRIPTION FACTOR-DNA

BINDING IN BIOSENSING APPLICATIONS

by

THUY THI HA NGUYEN

B.S., Boston University, 2015

Submitted in partial fulfillment of the

requirements for the degree of

Master of Science

2019

Approved by

First Reader   _____

                    Allison Dennis, Ph.D.
                    Assistant Professor of Biomedical Engineering
                    Assistant Professor of Materials Science and Engineering

Second Reader   _____

                    James E. Galagan, Ph.D.
                    Associate Professor of Biomedical Engineering
                    Associate Professor of Microbiology

Third Reader   _____

                    Mark W. Grinstaff, Ph.D.
                    Distinguished Professor of Translational Research
                    Professor of Chemistry
                    Professor of Biomedical Engineering
                    Professor of Materials Science and Engineering
                    Professor of Medicine

ACKNOWLEDGMENTS

FÖRSTER RESONANCE ENERGY TRANSFER (FRET)

AS AN OPTICAL READOUT FOR TRANSCRIPTION FACTOR-DNA

BINDING IN BIOSENSING APPLICATIONS

THUY THI HA NGUYEN

ABSTRACT

An alternative molecular recognition approach was developed for sensing small molecule analytes using the differential binding of an allosteric transcription factor (TF, specifically TetR) to its cognate DNA as the molecular recognition element coupled with Förster resonance energy transfer (FRET) to yield an internally calibrated optical signal transduction mechanism. Sensors were evaluated comprising Cy5-modified DNA (FRET acceptor) with either a tdTomato-TetR fusion protein (FP-TF) or quantum dot-TetR conjugate (QD-TF) as the FRET donor by measuring the ratio of acceptor and donor fluorescence intensities (F_A/F_D) with titrations of a derivative of the antibiotic tetracycline, anhydrous tetracycline (aTc). A proof-of-concept FRET-based biosensor was successfully demonstrated through the modulation of F_A/F_D signal intensities based on varying analyte concentrations. Sensor design parameters affecting overall signal-to-noise ratio and sensitivity of the sensors are also identified.

TABLE OF CONTENTS

LIST OF TABLES

LIST OF FIGURES

1. INTRODUCTION

1.1   Small Molecule Detection

Small molecules can be defined as low molecular weight organic molecules which are typically less than 1000 Da in size. This category includes a wide variety of compounds that are biologically, pharmacologically, or environmentally relevant, making the detection and quantification of these small molecules of great importance in many fields [6, 40]. For example, many small molecules are well-known contaminants in food and other agricultural products such as mycotoxins [7]. Mycotoxins are a diverse group of organic compounds produced by fungal species commonly found in cereals and nuts [47]. The negative health effects associated with mycotoxins are numerous, including their immunotoxicity, carcinogenicity, and nephrotoxicity [1, 13, 30].

On the other side of the spectrum, small molecules are of great interest in the pharmaceutical field for its potential in clinical medicine as well as in drug screening. In clinical medicine, small molecules can be advantageous with its intrinsic ability to cross the blood-brain barrier. Furthermore, the detection of many drugs is not only diagnostically and clinically relevant but also important for the development of new biotherapeutics and for studying the activity, kinetics, and stability of pharmaceuticals [18, 40].

Conventionally, many small molecules are detected by chromatographic methods such as high-performance liquid chromatography (HPLC) with UV and/or fluorescence detection (FLD) [22, 31, 46, 47]. These methods provide high sensitivity and specificity [44], but comes with major setbacks such as high cost, bulky instrumentation, and laborious

and time-consuming steps, making them not suitable for all applications. Biosensors can offer a cheaper and faster alternative [40].

Biosensors offer many advantages for the detection of small molecules including real-time monitoring, high specificity, rapid response, practicality, and convenience [34, 40]. Many biosensors and bioanalytical assays have been reported utilizing traditional enzyme-linked immunosorbent assays (ELISAs) [48, 49] and lateral flow strips [26] to fluorescent and electrochemical sensors [39].

1.2 FRET-based Small Molecule Biosensors

Generally, biosensors consist of a biorecognition element responsible for capturing the target analyte and a transducer, whose properties are altered upon analyte binding [43]. Optical transducers are based on measuring a change in optical properties in the presence of the analyte, such as absorption, reflectance, or emission, which can be recorded by a photodetector [17, 19, 29].

Optical biosensors offer many advantages such as high sensitivity, specificity, and the opportunity for real-time analysis [14]. Specifically, Förster resonance energy transfer (FRET) based biosensors have the advantages of high orthogonality, temporal resolution and ease of construction. FRET is a non-radiative dipole-dipole interaction that results in energy transfer from a donor molecule to an acceptor molecule. FRET efficiency is inversely proportional to the donor-acceptor distance to the sixth power [32]. This makes FRET a valuable tool for sensing nanometer scale changes in distance due to conformational changes and biomolecular binding.

FRET-based biosensors typically have a pair of donor and acceptor fluorophores

[50] with the ligand binding domain inserted in between. When the target molecule is bound, the ligand binding domain induces a conformational change, altering the distance of the donor and acceptor fluorophores and leading to a FRET signal change [3]. A wide variety of small molecules such as sugar phosphates [41], pyruvate [36], amino acids [28, 38]; and ions [25, 45] have been detected using FRET-based biosensors. In addition, FRET modulation of analyte binding offers the ability for ratiometric measurements, enhancing sensitivity. Both the emission intensities of the donor and acceptor can be monitored as well as the resulting changes in acceptor-donor emission ratios [8, 9].

1.3   Allosteric Transcription Factors as Biorecognition Elements

In addition to the choice of a transducer, the biorecognition element of a biosensor is highly critical. Antibodies continue to be one of the most used biorecognition elements due to their exceptional specificity and sensitivity. In addition, nucleic acids, aptamers, peptides, and molecularly imprinted polymers (MIPs) are also widely used [5]. However, these recognition elements require synthesis and optimization on a case-by-case basis for each small molecule of interest. This can become extremely labor-intensive, complex and expensive [2].

Bacteria have evolved over 3 billion years to respond to a wide range of stimuli. One mechanism of sensing is through an allosteric transcription factor. Transcription factors (TFs) are regulatory proteins that contain a DNA-binding domain and a ligand-binding domain. Transcription factors are able to recognize a wide variety of small molecules with high specificity and selectivity. In the presence of the target analyte, TF-DNA binding can be regulated, and therefore, possess an inherent transduction system.

This inherent transduction system has been exploited by many research groups for the development of whole cell biosensors [35], and molecular beacons for detecting DNA-binding proteins [23, 24]; yet, it has not been deeply explored for use in *in vitro* biosensors [33]. Recently, Yang et al. demonstrated the ability of utilizing isolated TFs as the molecular recognition element for sensing uric acid and oxytetracycline *in vitro*. They showed successful sensing by employing the amplified luminescent proximity homogeneous assay technology as the transducing element [33].

1.4   Rationale and Specific Aims

In this proposal, we explore the possibility of using FRET as the optical readout for TF-DNA binding by labelling the TF and DNA with fluorescent donor and acceptor molecules, respectively. When the TF and DNA are bound, the donor and acceptor molecules are in close enough proximity to enable FRET. This causes a decrease in donor emission, and an increase in acceptor emission. In the presence of the target analyte, the affinity of the TF for the DNA is greatly reduced, resulting in the unbinding of the TF-DNA complex. This results in the recovery of donor emission, and reduction in acceptor emission. By observing the analyte-induced changes in fluorescence of both the donor and acceptor molecules, we can obtain a ratiometric signal output to facilitate the quantification of the target analyte. The strong dependence of FRET on distance, however, can become the limiting factor on sensor sensitivity if the geometry and optical properties of the sensor components are not considered. Therefore, we also explore the differences in sensor performance with different donor molecules and configurations.

Specific Aim 1: Demonstrate feasibility of FRET as an optical readout of TF-DNA binding.

We will attempt to demonstrate the feasibility of utilizing FRET as the optical readout of TF-DNA binding by developing a model system utilizing a well-known and well-studied TF, TetR. It has been shown in literature that TetR specifically binds to a palindrome DNA sequence and unbinds the DNA in the presence of anhydrous tetracycline (aTc). The degree of unbinding of TetR is dependent on the concentration of aTc, which can be observed by the intensity of the observed FRET signal in the proposed biosensor.

We propose to use a recombinant fusion protein, TetR-tdTomato to serve as the FRET donor and Cy5-labelled DNA as the FRET acceptor. tdTomato and Cy5 were specifically chosen as a FRET pair due to their high spectral overlap and potential for high FRET efficiency. Furthermore, recombinant proteins can be easily expressed in E. coli at high yields and dye-labelled DNA are readily available commercially, making the production and assembly of the biosensor approachable. We expect to provide proof-of-concept data demonstrating the ability to detect and measure the modulation of TF-DNA binding in the presence of the analyte (aTc) via FRET.

Specific Aim 2: Characterize and optimize FRET system for improved sensitivity and signal output.

Upon demonstrating FRET as a viable sensor output, we will probe the effects of different FRET pairs on the biosensor's sensitivity and signal-to-noise ratio. We propose to introduce quantum dots (QDs) as one or both of the FRET molecules in the biosensor in an attempt to improve photostability, sensitivity, and signal intensity.

QDs have broadband absorption profiles and high molar extinction coefficients, making them efficient FRET donors and acceptors. Their broadband absorption allows for selective excitation of the donor molecule only (i.e. no direct acceptor excitation), reducing background noise. Increased brightness and photostability gained from QDs as compared to fluorescent proteins and dyes allows for the biosensor to be applied to a broader range of applications such as point-of-care diagnostics and continuous real-time sensing. We expect to pinpoint the critical parameters in our sensor design that can be tuned for the desired sensor sensitivity and dynamic range by comparing the effects of utilizing different sensor components.

2. MATERIALS AND METHODS

2.1   Quantum Dot Synthesis.

Cadmium oxide (CdO; 99.95%, Alfa Aesar), sulfur (99.95%, ACROS Organics), and 1-octadecene (ODE; 90%, ACROS Organics) were used as purchased from Fisher Scientific. Zinc acetate (99.99%), selenium (99.99%; pellets), oleic acid (OA; 90%), oleylamine (80%–90%), trioctylphosphine (TOP; 97%), and trioctylphosphine oxide (TOPO; *ReagentPlus®,* 99%) were used as purchased from Sigma-Aldrich. HPLC- grade solvents including hexanes (Fisher Scientific), methanol (Honeywell), chloroform (J.T. Baker), and ethanol (Sigma- Aldrich) were bought and used without further purification.

CdSe cores were nucleated using a modification of a previously described protocol [21]. Briefly, 1 g TOPO, 8 ml ODE, and 1.9 ml 0.2 M Cd(OA)$_2$ (1:4) were added to a 100 ml round bottom flask and degassed at room temperature for 30 mins. The flask was then heated to 80°C and degassed for another 30 mins. The temperature was raised to 300°C under argon atmosphere and a pre-mixed solution of 0.4 ml 1 M TOP:Se, 3 ml oleylamine, and 1 ml ODE was immediately injected into the flask. After 3 mins, the flask was removed from the heating mantle and cooled to room temperature on a cork ring. Once cooled, the raw QD core solution was transferred into an argon atmosphere glovebox and precipitated using a mixture of methanol and ethanol. After centrifugation, CdSe cores were re-suspended in hexanes and stored at 4°C under air-free conditions for future use.

A CdS shell was deposited on top of the CdSe cores using a modified successive ion layer adsorption and reaction (SILAR) method previously discussed [21]. For this, 5 ml ODE and 5 ml oleylamine were added to a 100 ml round bottom flask and degassed for

30 mins at room temperature and for an additional 30 mins at 80°C. Two hundred nmols of CdSe cores in hexanes were injected into the reaction flask and degassed for another 30 mins at 80°C. The core solution was heated to 160°C and enough cadmium oleate to coat the CdSe cores with a single atomic monolayer of material was added in the form of 0.2 M $Cd(OA)_2$ (1:4) in ODE. The reaction was maintained at 160°C for 1 hour before the temperature was raised to 240°C, where it was held for 1.5 hr. The same amount of sulfur was added in the form of 0.2 M sulfur dissolved in ODE and the reaction annealed for 1 hour. All subsequent injections and anneals were performed at 240°C with Cd and S anneals of 2.5 and 1 hours, respectively until the desired monolayers of CdS was reached. An additional 2 layers of ZnS was added on top of the QDs to passivate the surface in preparation of water solubilization. The same SILAR method was used as above, but with 0.2 M $Zn(OA)_2$ (1:4) as the cation precursor and 1 hour anneal times for both Zn and S additions.

The core/shell/shell QDs were then precipitated out of solution to remove any excess reagents using a mixture of methanol and ethanol. TEM images were taken to determine size distribution. QDs were transferred to water using a zwitterionic ligand CL4 previously described [42]. Quantum yield measurements were taken using an integrating sphere attachment on the Horiba Nanolog.

2.2   CL4 Ligand Synthesis.

DL-Thioctic acid (≥98%; ACROS Organics), 1,1′-carbonyldiimidazole (CDI; 97%, ACROS Organics), methyl acrylate (≥99%, ACROS Organics), sodium borohydride (NaBr4), and silica gel sorbent (230-400 mesh, grade 60) were purchased from Fisher

Scientific. Ethylenediamine (≥99%), lithium hydroxide (LiOH; ≥98%), hydrochloric acid (HCl; 37%), and sodium hydroxide (NaOH; 50% in H2O) were purchased from Sigma-Aldrich.

A short zwitterionic ligand, compact ligand four (CL4) developed by Susumu et al. was used to water solubilize the QDs [42]. The ligand was synthesized with modifications as previously described [9]. Briefly, 12 g (0.0145 mol) of thioctic acid and 10.36 g (0.064 mol) of CDI were added to a 250 mL round bottom flask and purged with argon. 120 mL of chloroform was added by syringe and the mixture was stirred for 1 hr at room temperature under argon. The solution was then added dropwise into a pre-mixed solution of 32 mL of ethylene diamine and 120 mL of chloroform via an additional funnel under argon atmosphere over the course of 4 hrs with stirring. The mixture was left to stir at room temperature overnight. The organic phase was collected using a separatory funnel and the aqueous phases was washed an additional three times with chloroform.

The organic layers were pooled and concentrated to ~80 ml on a rotary evaporator to be purified on a silica gel column (CHCl$_3$/MeOH (5:1) eluent). The purified crude product was concentrated under vacuum to ~60 mL and diluted with 280 mL MeOH. 40 mL of methyl acrylate was added dropwise and the resulting solution was left to stir for 2 days under active argon flow at room temperature. The excess methyl acrylate and solvent was evaporated off and the product was again purified on a silica column with CHCl$_3$/MeOH (20:1) as the eluent instead. The purified product was concentrated to a yellow oil. The product was weighed and stored at 4°C for subsequent ring-opening immediately prior to QD ligand exchange.

To ring open the stored product, 20.9 mg LiOH, 2 mL EtOH and 1 mL DI H2O was added for every 0.321 g of product. The mixture was allowed to react for 2 hours at room temperature before 4 M HCl was used to adjust the pH of the solution to ~8. For every 0.321 g of product, 60.6 mg of $NaBH_4$ was added and the solution was allowed to stir at room temperature for an additional 1.5 hrs. The pH of the solution was adjusted to ~7-8 and filtered through a cotton plug to remove excess salts and unreacted materials. Excess EtOH was evaporated off and the clear liquid was stored at 4°C for ligand exchange. A biphasic mixture of QDs in chloroform and CL4 in water was left to stir overnight under argon filled glass vials. The ratio of CL4 to QD was adjusted based on QD surface such that 2000 molecules of CL4 per unit surface area (nm^2) of QD was used in each transfer.

2.3   Protein Expression and Purification.

NEB® 5-alpha (Cat# C2987I) and BL21(DE3) (Cat# C2527I) competent *Escherichia coli* cells were purchased from New England Biolabs and used to replicate and express plasmids, respectively. LB broth (Lennox; powder), kanamycin sulfate (mixture of Kanamycin A (main component) and Kanamycin B and C; powder), isopropyl b-D-thiogalactopyranoside (IPTG; ≥99%), phosphate buffered saline, pH 7.4 (PBS; packets), and lysozyme from chicken egg white (~7000 U/mg; powder(crystalline)) were purchased from Sigma-Aldrich. Dextrose (granules (crystalline)), Halt™ protease inhibitor cocktails (100X) were purchased from Fisher Scientific. 1,4-Dithiothreitol (DTT; >99% (protease-free)) was bought and used as is from Gold Biotechnology (St. Louis, MO). Nickel-nitrilotriacetic acid (Ni-NTA) agarose resin and Strep-tactin® Superflow Plus resin were purchased from Qiagen (Germantown, MD) for affinity-tag chromatography purification

of proteins. Strep-tactin® Purification Buffer Set was purchased from IBA (Gottingen, Germany). Sodium phosphate (NaH$_2$PO$_4$; ≥98%, monobasic monohydrate), sodium chloride (NaCl; BioXtra, ≥99.5%), and imidazole (≥99%) were purchased from Sigma for buffer preparation used with Ni-NTA agarose resin.

Acrylamide/Bis-Acrylamide (37.5:1) 40% (w/v) solution (BioBasic, ON, Canada), glycine (≥99%, Sigma-Aldrich), N,N,N',N'-tetramethylethylenediamine (TEMED; ~99%, Sigma-Aldrich), ammonium persulfate (APS; ≥98%, Sigma-Aldrich), SDS-PAGE protein standards, broad range (unstained, Bio-Rad), tris(hydroxymethyl) aminomethane (ultra pure, Research Products International (RPI)), sodium dodecylsulfate (SDS; powder, RPI), bromophenol blue (Sigma-Aldrich), 2-mercaptoethanol (BME; ≥99%, Sigma-Aldrich), glycerol (≥99.5%, Fisher Scientific), Coomassie Brillant Blue G (250, Sigma-Aldrich), and acetic acid (glacial, J.T.Baker) were purchased for SDS-PAGE protein molecular weight verification. Protein assay kit II (Bradford reagent) was purchased from Bio-Rad for protein quantification.

Plasmids encoding the gene for His-tagged tetR(C) and tetR(D) (tetR(C),tetR(D)) and Strep-tagged fusion protein tetR-tdTomato were generously provided to us by the Galagan Lab. Escherichia coli BL21(DE3) were transformed with plasmids following standard molecular biology techniques. Cells were grown at 37ºC in LB broth supplemented with a final concentration of 0.4% glucose and 33ug/ml kanamycin. Protein expression was induced at an OD600 between 0.5 – 1 by adding IPTG to a final concentration of 1 mM. The temperature was lowered to 30ºC and cultures were incubated for 4 hours. Cells were harvested by centrifugation, re-dispersed in 10 mM PBS, 1 mM

DTT, 1X Halt protease inhibitor cocktail, and stored at -80ºC until purification. The fusion protein TetR-tdTomato was also expressed following the above methods with the exception of an overnight induction with IPTG.

For purification, a final concentration of 1 mg/ml lysozyme was added to the thawed whole cell lysate and allowed to incubate for 1 hour at 4°C. Soluble proteins were obtained by centrifugation at 4ºC for 30 mins at 18,000 rpm. Cleared cell lysates were purified using a Strep-tactin column for the TetR-tdTomato fusion protein and a Ni-NTA column for the TetR-6His proteins. Fractions were collected from the affinity columns and analyzed using a 10% and 15% SDS-PAGE gel for TetR-6His proteins and TetR-tdTomato, respectively. Fractions containing the protein of interest were pooled, concentrated and buffer exchanged into TBS via 10 kDa and 50kDa centrifugal filters for TetR-6His proteins and TetR-tdTomato, respectively (Amicon). Concentrations were determined using a Bradford assay as well as UV spectroscopy using the molar extinction coefficient of tdTomato (138,000 M^{-1} cm^{-1}). Protein stocks were aliquoted and stored at -80C in 25% glycerol and 1 mM DTT until further use.

2.4   DNA Hybridization.

The synthetic 28bp tetO-containing oligonucleotide with modified 5'- and 3'-Cy5 and its complement were purchased from IDT and hybridized to generate double-stranded fluorescent probes. Equal molar amounts of each oligonucleotide were mixed with 1X nuclease-free duplex buffer (30 mM Hepes pH 7.5, 100 mM KAc, IDT), heated to 95ºC for 2 mins and allowed to cool down to room temperature wrapped in aluminum foil to prevent photo-oxidation of the Cy5 dye. A scrambled non-binding oligonucleotide

sequence was also purchased and hybridized as above for a negative control.

2.5 FRET Assays.

Bovine serum albumin (BSA; DNase- and protease-free, Fisher Scientific), tris-hydrochloride (Tris-HCl; ≥99%, Promega), magnesium chloride hexahydrate (MgCl$_2$; ≥99%, Sigma-Aldrich), salmon sperm DNA solution (UtraPure™, Invitrogen), and anhydrotetracycline hydrochloride (aTc; Alfa Aesar) were used as purchased.

Sensors were prepared in a solution of TBS + 0.2% (w/v) BSA and 1X binding buffer (20 mM Tris-HCl, 5 mM MgCl2, 5% glycerol, 50 ng/µl salmon sperm DNA). To prepare the tdTomato sensor, tetR-tdTomato and Cy5-modified DNA were allowed to incubate at a 1:3 ratio. The sensor solution was pipetted into wells of a black, non-binding 384-well plate. aTc was added into each well such that the final concentrations of the components were 200 nM tetR-tdTomato, 600 nM Cy5-modified DNA, and 0-675 nM aTc with a final volume of 60ul. For triplicate measurements, each of the above solutions were prepared with a final volume of 180 µl in microcentrifuge tubes and pipetted into 3 separate wells of 60 µl each.

To prepare the QD sensor, QDs and TetR-6His were allowed to incubate at a 1:4 ratio to allow for the tetR-6His to self-assemble on the surface of the QDs [11]. The QD-tetR conjugates were then incubated with the Cy5-modified DNA at a 1:4.5 ratio. The final ratios between the QD, tetR-6His, and Cy5-modified DNA were 1:4:18, respectively. aTc was added to the wells above with final concentrations of 50 nM QDs, 200 nM tetR-6His, 900 nM Cy5-modified DNA, and 0-2700 nM aTc.

Emission spectra were taken with the MicroMax plate reader attachment on the

Horiba Nanolog fluorimeter with tetR-tdTomato excitation set at 500nm and QD excitation set at 400nm with a slit width of 2nm and 3s integration time per well. Negative controls were prepared exactly the same way using a Cy5-modified scrambled DNA sequence as the acceptor to account for collisional quenching of the donor.

2.6   FRET Analysis.

The overlap integral J, describes the spectral overlap of the donor emission and acceptor absorbance according to the following equation:

$$\mathbf{J} = \int \overline{\mathbf{F_D}}(\lambda)\boldsymbol{\varepsilon_A}(\lambda)\lambda^4 d\lambda, \tag{1}$$

where $\overline{\mathbf{F_D}}(\lambda)$ is the normalized donor emission spectrum and $\boldsymbol{\varepsilon_A}(\lambda)$ is the molar extinction coefficient of the acceptor as a function of wavelength λ. The Förster distance $\mathbf{R_0}$ is defined as the donor-acceptor distance at which 50% FRET efficiency is observed as described by:

$$\mathbf{R_0^6} = (\mathbf{0.02108})\boldsymbol{\kappa}\mathbf{Q_D}\frac{\mathbf{J}}{\boldsymbol{\eta^4}}, \tag{2}$$

where $\boldsymbol{\kappa}$ is 2/3 under the assumption of random dipole orientation, $\mathbf{Q_D}$ is the donor quantum yield, and $\boldsymbol{\eta}$ is the solvent refractive index [10].

2.7   Sensor Analysis.

Raw spectral data were background subtracted for direct acceptor excitation and peak-fitted using OriginPro. The ratio of the areas of acceptor emission over donor emission (F_A/F_D) using the integrals of the peak emissions were calculated and plotted to determine the linear and dynamic ranges of the sensors.

To compare between the different sensors, the data were normalized to the no aTc controls and fitted to the following logistic function to determine EC50:

$$y = A_2 + \frac{(A_1 - A_2)}{1 + \left(\frac{x}{x_0}\right)^p} \, , \qquad (3)$$

where A_1 is the initial value, A_2 is the final value, x_0 is the concentration at which there

is 50% signal, and p is the Hill coefficient.

3. RESULTS AND DISCUSSION

By exploiting the difference in the binding affinity between the TF and its specific binding sequence in the presence and absence of a small molecule analyte, the TF-DNA binding and unbinding becomes a sensor for the small molecule effector (**Figure 1**). The transcription factor TetRc was used for this proof-of-concept sensing study because it is a well characterized allosteric TF that is used extensively for gene regulation and inducible protein expression in the laboratory setting.

TetRc binds to the *TetO* DNA sequence in the absence of the effector molecule anhydrous tetracycline (aTc). The *TetO* cognate sequence comprises a 19 bp binding region. In the sensor design, the 19 bp cognate sequence was flanked by 4-5 bp on each side to ensure binding, resulting in a 28 bp DNA oligo. One of the strands was labeled with the FRET acceptor Cy5 on both the 5' and 3' ends. A second 28 bp sequence with no affinity for TetR was similarly labeled to act as the negative control (**Table 1**).
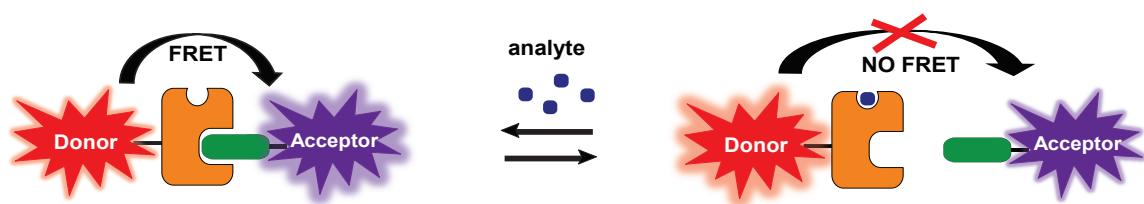
Figure 1. Schematic of generalized FRET sensor using TF-DNA binding mechanism. Binding of the TF to a specific DNA sequence brings the donor and acceptor fluorophores into close proximity, enabling Förster resonance energy transfer (FRET). Upon binding of the effector analyte, the affinity of the TF for the DNA binding sequence is significantly reduced, resulting in unbinding of the TF-DNA complex. Therefore, energy transfer to the acceptor is minimal resulting in higher donor emission and lower acceptor emission intensities. Schematic not to scale.

Table 1. Synthetic DNA oligos for TetRc binding.

Name	Sequence [a]
TetO^4 (forward)	5'-GTCA **TCCCTATCATTGATAGAGA** TACTG-3'
TetO' (reverse)	3'-**C**AGT **AGGGATAGTAACTATCTCT** ATGA**C**-5'
Scrambled (forward)	5'-TCGT GAAACCGAGCGAGGGACAC GCACA-3'
Scrambled (reverse)	3'-**A**GCA CTTTGGCTCGCTCCCTGTG CGTG**T**-5'

[a] The *TetO* binding sequence is the center region shown in blue; nucleotides labeled with Cy5 dye are labeled in red and underlined.

3.1 *The Effects of Different FRET Donors on Sensor Performance*

Two FRET-based sensors utilizing the TF-DNA binding mechanism were developed and characterized for the sensing of the small molecule aTc. Different FRET donors were used in order to investigate the effects of FRET efficiency and multi-valency on overall sensor performance. Each sensor consists of Cy5-modified DNA acting as the FRET acceptor with either a fluorescent protein-transcription factor (FP-TF) fusion protein (expressed in *E. coli*) or quantum dot-transcription factor (QD-TF) conjugate as the donor. The spectral overlap between the respective donor emission peaks and the Cy5 absorption for each sensor is shown in **Figure 2A** and **Figure2C**. The QD-Cy5 FRET pair exhibits increased spectral overlap compared to tdTomato (**Table 2**). The much higher quantum yield of tdTomato compared to the QDs, however, results in a larger calculated Förster distance, R_0, for the tdTomato-Cy5 FRET pair than the calculated R_0 for the QD-Cy5 FRET pair (**Table 2**). Thus, we would expect that in 1:1 donor: acceptor pairs with the same donor-acceptor distances, the tdTomato-Cy5 sensor would exhibit the most efficient energy transfer.

Table 2. FRET Calculations.

Donor	QY (%)	J (x 10^{16} M^{-1} cm^{-1} nm^4)	R_0 (nm)
TetRc-tdTomato	69	1.34	7.43
CdSe/4CdS/2ZnS QDs	23.4	2.69	6.96

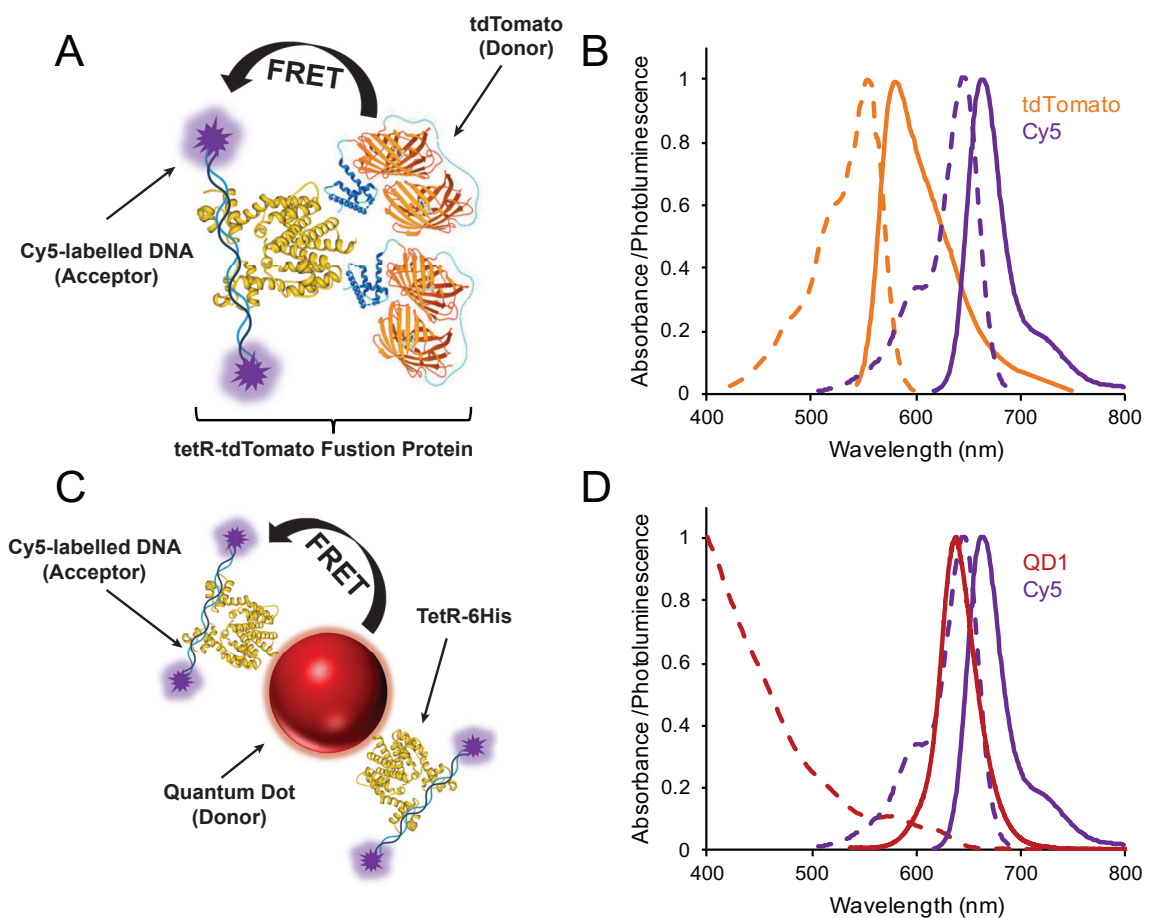| Acceptor	Molar Extinction Coefficient (M^{-1} cm^{-1})
Cy5	250,000

Figure 2. Absorbance (dashed lines) and emission (solid lines) spectra of tdTomato **(B)** and QD **(D)** overlapping Cy5. Schematics of the FP-based **(A)** and QD-based **(C)** sensors highlight the differences in sensor geometry. The QD-based sensor allows the ability for multiple acceptors per donor whereas the FP-based sensor is inherently a 1:1 ratio.

While as-synthesized QDs can exhibit near unity QYs [20], the thiolate-based ligands that produce the smallest possible organic coating on the semiconductor surface for water solubility are widely known to significantly quench the QD photoluminescence due to the introduction of surface trap states [16, 38]. The thin organic coating is desirable both to reduce donor-acceptor distance and to facilitate histidine-tag-mediated self-assembly of the proteins to the QD surface [38]. Previous results from our lab have shown that a moderately thick shelled core/shell QD heterostructure can be used to improve the QD QY following ligand exchange while moderating the distance added between the donor and acceptor molecules for efficient energy transfer [9]. In this context, core/shell/shell QDs were utilized comprising of CdSe/4CdS/2ZnS, where the number before the shell composition indicates the number of atomic monolayers that were deposited on the core. The diameter of the semiconductor QD based on TEM imaging is 7.6 ± 1.1 nm while DLS of the water-soluble particles indicates a hydrodynamic diameter of 10 ± 2 nm, showing the minimal increase in size from the CL4 ligand coating.

Despite the less favorable Förster overlap, the nanoparticle-based sensor has the advantage of multi-valency. Specifically, multiple his-tagged TFs can self-assemble stoichiometrically with a Poissonian distribution of proteins onto the QD surface [10, 15]. This enables the binding of multiple acceptor dye-labeled oligos to a single QD donor (**Figure 2D**). Adding multiple acceptor molecules has the benefit of increasing the FRET efficiency compared to a single acceptor at the same donor-acceptor distance. In contrast, a greater number of donors per acceptor reduces FRET efficiency (**Figure 3**) [10, 15].
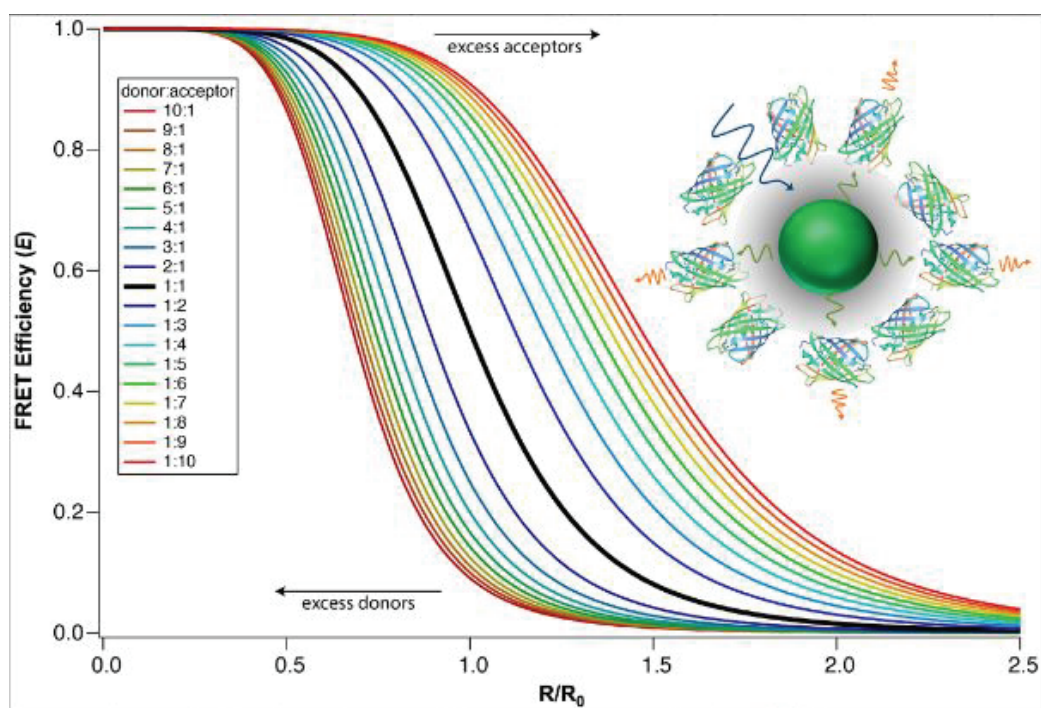
Figure 3. Distance dependency of FRET efficiency for multivalent systems. FRET efficiency increases as the number of acceptors per donor increases. In contrast, the presence of excess donors decreases FRET efficiency. Reproduced from [10].
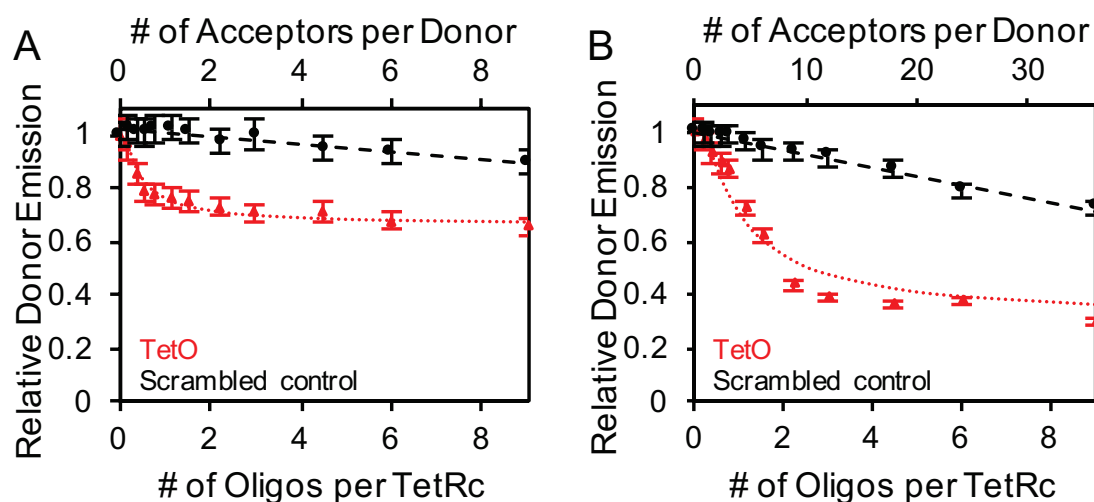
Figure 4. Relative donor emission plots as a function of molar acceptor ratios using **(A)** tdTomato and **(B)** QDs as FRET donors. Ratios of donor to TF was fixed at 1:1 for the tdTomato-Cy5 sensor and 1:4 for the QD-Cy5 sensor. Controls (black) use a scrambled oligo sequence with no affinity to TetR to measure the collisional quenching. Data are mean +/- standard deviation for n = 3.

Binding of the Cy5-modified DNA to the TetR-modified donors was demonstrated by titrating increasing concentrations of the DNA; the donor concentration was adjusted to keep overall TF concentration constant at 200 nM. Upon increasing DNA concentration, there is increased donor quenching in both cases. The non-linear response to increasing acceptor concentration is seen, as is characteristic of FRET systems. The results were plotted using a modified Hill equation, as previously described [34]. There is less donor quenching when titrating a non-binding DNA sequence at the same concentrations, demonstrating specific binding and donor quenching (**Figure 4**). The linear response from the non-binding control is described by Stern-Volmer collisional quenching [15, 34]. Calculated FRET efficiencies demonstrate that the QD-Cy5 sensor exhibits a higher FRET efficiency (50%) compared to the tdTomato-Cy5 sensor (30%). These results agree with the hypothesis that the nanoparticle-based sensor would exhibit a higher FRET efficiency due to its inherent ability for multi-valency compared to TetR-tdTomato when the binding affinity of the TF to DNA is kept constant, despite having a lower calculated R_0 value.
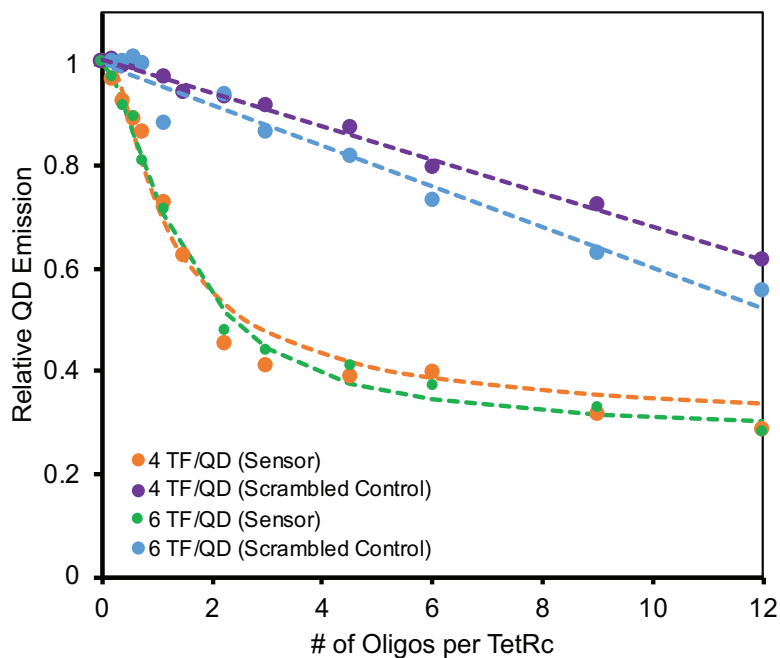
Figure 5. Relative QD emission plots as a function of DNAs per TF for both 4 TFs/QD and 6 TFs/QD ratios.

The QD-based sensor was tested with 6 TFs per donor to determine if the FRET efficiency of the system could be increased. As shown in **Figure 5**, increases from 4 to 6 TFs per QD did not significantly improve FRET efficiency. Thus, four his6-TetRc monomers were used per QD for subsequent sensor designs. Inherently, the ratio of fluorophores:TF is fixed at 1:1 for the TF-FP fusion protein-based sensor.

A TF to DNA ratio was chosen for each sensor (3:1 for tdTomato, 4.5:1 for QDs) and kept constant for subsequent experiments testing sensor sensitivity to aTc. Photoluminescence spectra measured from sensors with increasing concentrations of aTc yielded changes in the ratio between the acceptor emission and donor emission (F_A/F_D). With increasing concentrations of aTc, the F_A/F_D values decreased indicating unbinding of the DNA from the TF, resulting in a recovery of donor emission and decrease in acceptor

emission (**Figure 6**). No changes were observed when aTc was titrated into a solution of non-binding donor-acceptor pairs (scrambled controls). This indicates the specific recovery of donor emission (and reduction in acceptor emission) due to TF-DNA unbinding.
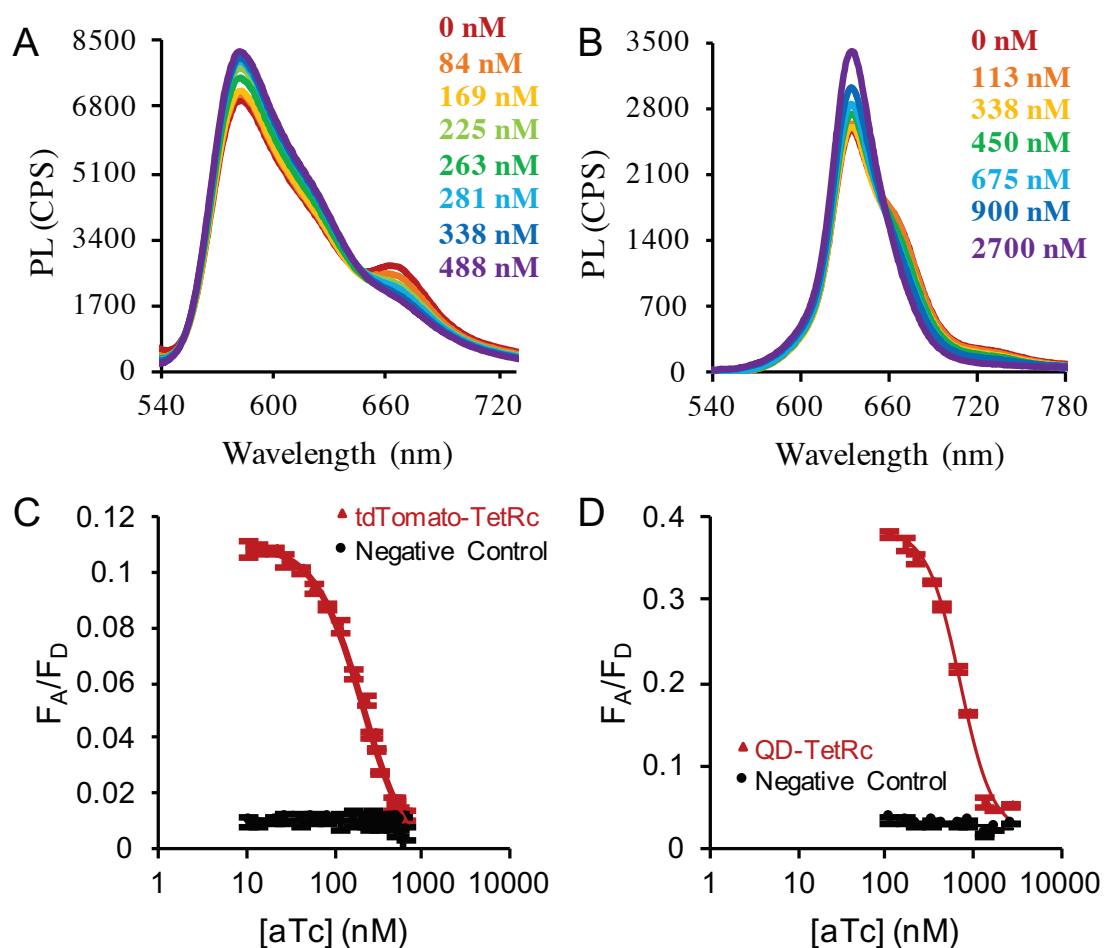
Figure 6. (A, B) Representative spectral data of the sensors (TetR-tdTomato, QD-TetR) in response to aTc concentration. Recovery of donor fluorescence intensities in response to higher aTc concentrations demonstrate modulated unbinding of the DNA from the TF. **(C, D)** Ratio of acceptor fluorescence to donor fluorescence (F_A/F_D) as a function of aTc concentration. tdTomato sensor was prepared with a 1:1:3 ratio of tdTomato:TF:DNA whereas the QD sensor was prepared with a 1:4:18 ratio of QD:TF:DNA. tdTomato (200nM) and QD (50nM) concentrations were selected to keep TF concentration constant at 200nM. Data are mean ± standard deviation for n=3.

Table 3. Summary of Logistic Fit Coefficients.

Sensor	E_{sensor}	EC50(nM)	h	Signal-to-Noise Ratio
tdTomato-Cy5	0.300	218 ± 9.18	1.57 ± 0.0802	6.20
QD-Cy5	0.500	699 ± 26.4	2.37 ± 0.191	13.9

Comparing sensor outputs during the titration of aTc revealed an inverse relationship between FRET efficiency and sensor sensitivity. The tdTomato-Cy5 sensor exhibited higher sensitivity compared to the QD-Cy5 sensor. This implies that the overall degree of acceptor unbinding in the presence of aTc defines the sensor's sensitivity. The inherent 1:1 donor: acceptor ratio of the tdTomato-Cy5 sensor allows for the sensor components to exist only in two states at equilibrium when aTc is present: (1) TetRc-tdTomato bound to Cy5-DNA and (2) TetRc-tdTomato unbound to Cy5-DNA. This allows for a much greater change in signal intensity between the two states. On the other hand, the multi-valency of the QD-Cy5 sensor allows for four different binding states from Cy5-DNA and QD-TetRc being completely unbound to Cy5-DNA occupying all four binding sites of the QD-tetRc conjugate. The ability for the sensor to exist in multiple bound states hinders its sensitivity. A greater number of aTc molecules are required to transition between the maximum and minimum FRET states for the QD-based sensor as compared to the FP-TF-based sensor. In compromising on sensitivity, the QD-based sensor exhibited a higher signal-to-noise ratio, which can be beneficial in applications requiring benchtop devices. The next section of this work aims to explore the ability to improve the sensitivity of the QD-based sensor by changing the inherent affinity between the TF and DNA.

3.2   The Effects of Affinities between TF and DNA on Sensor Sensitivity

Yang et al. demonstrated that the limit of detection of their transcription factor-based sensor could be lowered by introducing point mutations into the its binding sequence. The point mutations lowered the affinity of the DNA to the TF, and thereby increasing sensitivity of the sensor in the presence of the effector analyte [33]. Fields et al. identified variants of the *tetO* sequence with differential affinity and therefore, resulting in different activator-driven expression levels [12]. They identified several *tetO* variants with activity levels ranging from 5% to 85% as compared to the wild-type sequence. We chose 3 of the *tetO* variants identified by Fields et al. with activity levels of 70%, 30% and 5% as compared to the wild-type to test with our QD sensor (**Table A1**). Theoretically, by reducing the affinity of the DNA for the TF, fewer effector molecules would be required to transition from the maximum and minimum binding states, thus, increasing sensitivity. All ratios and conditions for the sensor were kept the same as previously mentioned.

Due to the lower binding affinity of the DNA to the TF, the signal-to-noise of the sensor decreases as the activity levels of the Cy5-DNA decreases (**Figure 7A**). This is directly related to the overall FRET efficiency of the system. Fewer initial binding events due to the lower affinity of the DNA to TF leads to fewer number of donor-acceptor pairs contributing to FRET. A normalized plot of the sensor response curves reveals, however, that there are no significant changes in the sensor's sensitivity to aTc (**Figure 7B**).
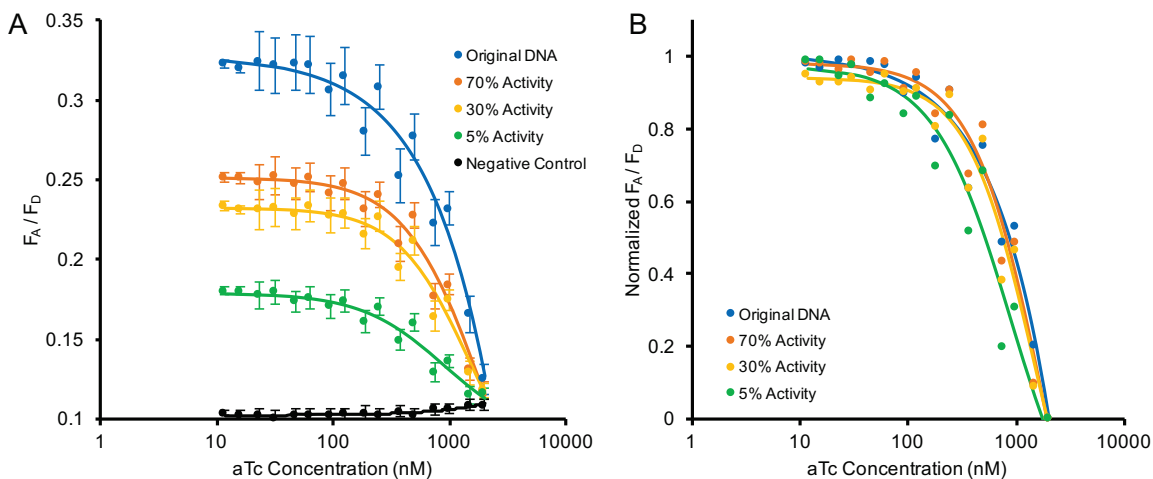
Figure 7. (A) Response curves of the QD-TetRc sensor with Cy5-DNA of varying activity levels. Signal-to-noise ratio of the sensor decreases as activity levels of the Cy5-DNA decreases. **(B)** Normalized F_A/F_D plot of the different QD-TetRc sensors reveals no significant change in aTc sensitivity.

There are a few possible explanations for these results. As mentioned, Fields et al. were able to identify the *tetO* variants based on the expression levels of the LUC1 gene as determined by luciferase activity [12]. The K_D of the *tetO* variants to TetRc was not directly measured. Although binding affinities play a heavy role, there are many confounders that can affect expression levels. The activity levels of the *tetO* variants may not be directly proportional to its binding affinity. Another explanation could be in the sensor configuration. During these assays, the ratios between the QD, TF, and DNA were kept constant based on previous results. Changing the ratios between these components could force the majority of donor-acceptor pairs into one of the different binding states instead. For example, a 1:1 ratio of QD:TF could be used to obtain a similar configuration to the TetRc-tdTomato, where only two binding states are possible. This increases sensitivity as previously shown. However, the Poissonian distribution of TF his-tagged binding should also be taken into consideration since unlabeled donors could hinder the overall detectable

signal of the sensor.
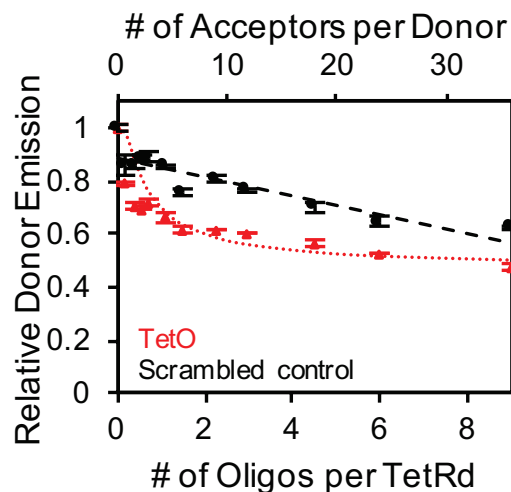
Figure 8. Relative QD emission plot as a function of molar acceptor ratio using the TetRd protein variant.

An alternative to adjusting binding affinities via the DNA sequence is to modify the TF itself. Many mutations of TetR are known to change its responsivity to the analyte; for example, revTetR reverses the binding mechanism causing TF-DNA binding in the presence of aTc rather than its absence [27]. The variant TetRd was identified from literature and used in subsequent studies to determine the ability of tuning the sensor output by subtly modifying the binding affinity of the TF to its DNA oligo. A QD with comparable spectral properties was also used in these studies for comparison (**Figure A1, Table A2**).

Titration of Cy5-modified DNA into the QD-tetRd conjugate confirmed binding of the TetRd protein variant to the *tetO* sequence (**Figure 8**). However, the FRET efficiency is greatly reduced (15%) compared to the QD-TetRc (40%) and TetRc-tdTomato (30%). With similar sensor properties (i.e. spectral overlap, donor-acceptor distances, etc.), the lower FRET efficiency implies a lower binding affinity of TetRd to its DNA compared to TetRc.
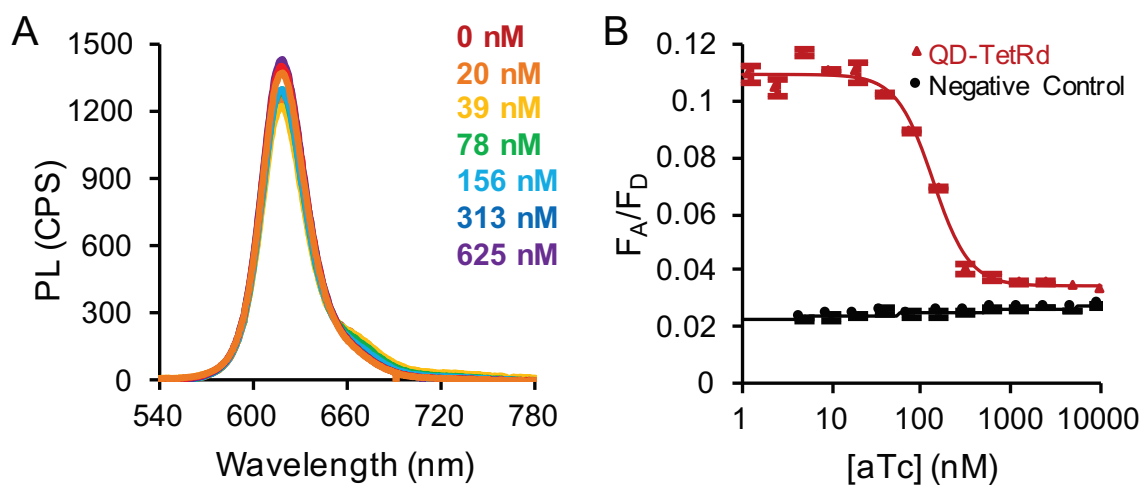
Figure 9. (A) Representative spectral data of QD-tetRd sensor in response to increasing concentrations of aTc. **(B)** F_A/F_D plot of the QD-tetRd sensor as a function of aTc concentration.

The aTc response curves of the QD-TetRd sensor revealed an EC50 of 133 ± 6.15 nM, a 5-fold decrease compared to the QD-TetRc sensor (EC50 = 699 ± 26.4 nM) and roughly 1.6-fold decrease compared to the TetRc-tdTomato sensor (EC50 = 218 ± 9.18 nM) (**Figure 9**). This further supports the notion that FRET efficiency is inversely proportional to sensor sensitivity. The significant increase in sensitivity, however, comes with a large decrease in the signal-to-noise ratio (3.60) (**Figure 9**). Normalized plots of all three sensors utilizing the TetR protein are shown in **Figure 10** for easy comparison.
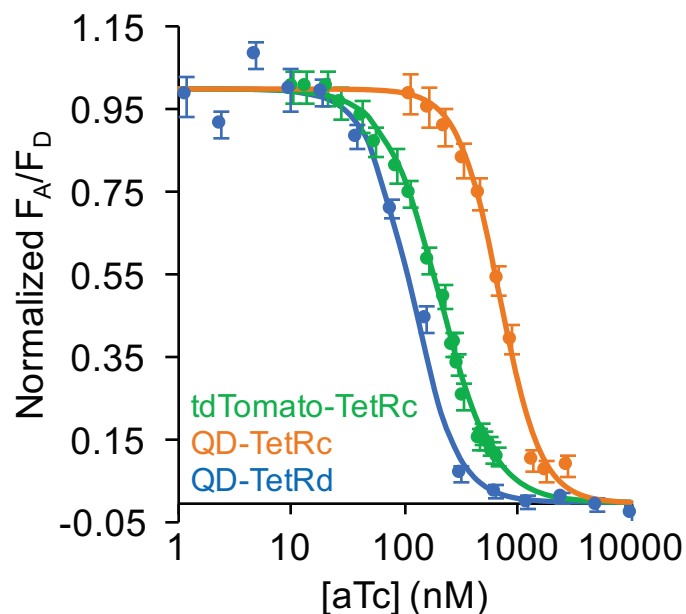
Figure 10. Normalized F_A/F_D plots of the FRET-based sensors using the TetR transcription factor as a function of aTc concentration.

We have generated proof-of-concept data showing that FRET is a valid optical readout for observing the binding and unbinding of a TF to its DNA sequence in the presence of its effector molecule. Furthermore, we have demonstrated the ability to alter the sensitivity of the sensor by modifying the TF and changing its affinity for the DNA. This increase in sensitivity, however, comes with a sacrifice in the signal-to-noise ratio of the overall sensor. The next part of this work aims to apply this sensor scheme using a different TF that is responsive to a clinically relevant molecule of interest.

3.3   Applying Sensor Design to Clinically Relevant TF

We have shown that the TF-DNA binding mechanism can be exploited for analyte sensing using FRET. To further validate the QD sensor scheme, we tested the design using another TF of interest. A previously uncharacterized TF, AIY20223.2 (AIY), that is

responsive to progesterone and its binding sequence were identified and isolated by the Galagan group. Specific binding of the TF was shown by titration of the Cy5-modified DNA in increasing concentrations (**Figure 11**). The QD:TF:DNA ratio was kept constant at 1:4:18 as in previous studies. The calculated FRET efficiency of this system was 18%.
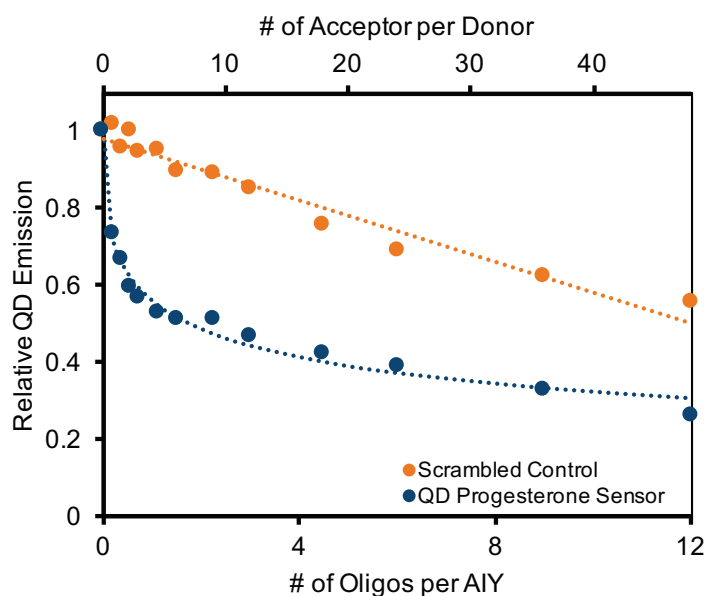
Figure 11. Relative QD emission plot of the QD-AIY sensor as a function of molar acceptor ratio.

Since AIY is known to be responsive to progesterone, we were curious to see if AIY was specific to progesterone or generally responsive to steroid hormones. Therefore, the QD-AIY sensor was tested with a variety of steroid hormones such as aldosterone, estrone, and estradiol in addition to progesterone. As shown in **Figure 12**, the QD-AIY sensor was highly responsive to progesterone and showed no response to estrone, or estradiol. There was, however, some cross reactivity with aldosterone, albeit with a much higher EC50 of 4660 ± 614 nM compared to an EC50 of 577 ± 30.0 nM for progesterone. We also revisited the possibility that changing the ratio of TF to QD could affect its

sensitivity. In earlier studies, we tested a higher ratio of TF to QD in order to maximize

FRET efficiency; however, our studies have shown that higher FRET efficiency does not

result in higher sensitivity, but quite the opposite. Ratios of 3, 4, and 5 TFs per QD were

tested and the normalized results are shown in **Figure 13**. No significant changes in

sensitivity to progesterone were seen. More work should be done to probe the specific

binding kinetics of AIY, its DNA, and progesterone to get a better understanding of which

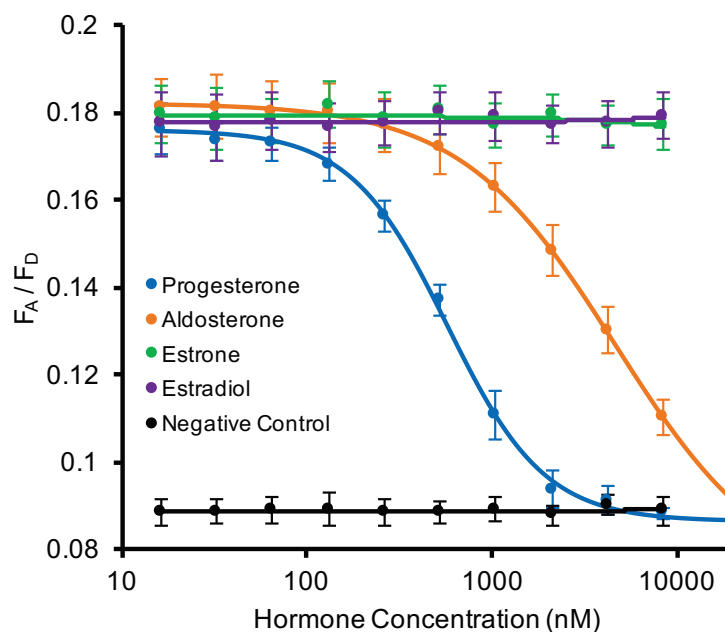parameters are most important for tuning sensor performance.

Figure 12. F_A/F_D plots of the QD-AIY sensor as a function of concentration of various steroid hormones. The response curves indicate some cross reactivity of the AIY to aldosterone.
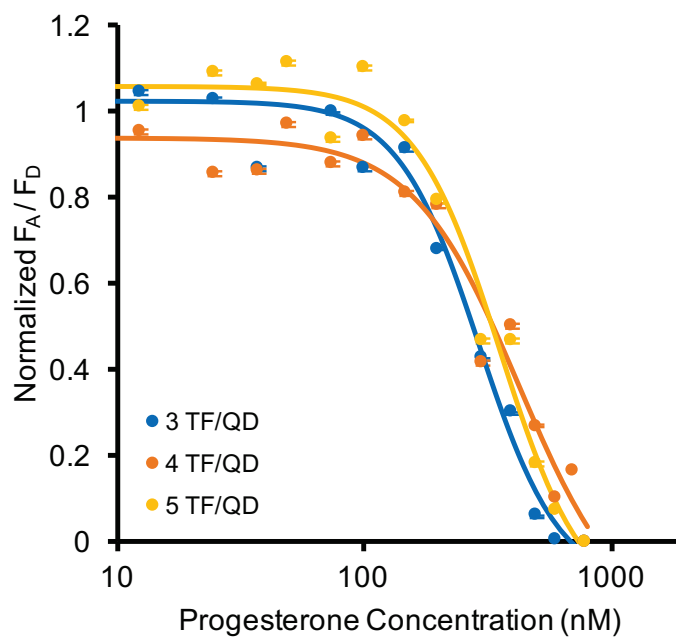
Figure 13. Normalized sensor response curves as a function of progesterone concentration of QD-AIY sensors with varying TF to QD ratios.

4. CONCLUSIONS AND FUTURE WORK

We have shown that this TF-DNA binding mechanism is a reliable molecular recognition element in sensing applications and have successfully shown that FRET is a valid optical readout for observing the binding and unbinding of a TF to its DNA in the presence of an effector molecule. FRET can be effectively used with the TF-DNA binding mechanism regardless of donor-acceptor pairs. We have demonstrated the importance of selecting the appropriate donor-acceptor pair for the desired application. If a high signal-to-noise ratio is required to be detected by off-the-shelf detectors, the QD-based sensor may be a better choice over the lower detection limit of the FP-based sensor and vice versa. Moreover, we have displayed the ability to tune sensor performance by altering the affinity of the TF for its DNA and the versatility of this sensor design as a whole. The modularity of the sensor allowed us to use an entirely different TF to detect and measure a molecule of interest.

Because there were compromises in signal intensities of the sensors with respect to sensitivity for the multivalent QD systems, the configuration and ratios of the sensor components should be investigated further. Since it has been demonstrated that this sensor design scheme works regardless of donor-acceptor pairs, it would also be interesting to explore additional FRET pairs in future work.

APPENDIX

Table A1. Alternative DNA sequences for TetR with varying activity levels.

Name	Sequence [a]
Original DNA (wt-*tetO*)	5'- **C**AGTATCTCTATCAATGATAGGGATGA**C** -3'
70% Activity	3'- **C**AGTATCTCTATCAATGATA**C**GGATGA**C** -5'
30% Activity	5'- **C**AGTATCTCTATCAATGA**G**AGGGATGA**C** -3'
5% Activity	5'- **C**AGTATCTCT**G**TC**C**ATGATAGGGATGA**C** -3'

Table A2. FRET Calculations for QD2 used in AIY sensor.

Donor	QY (%)	J (x 10^{16} M^{-1} cm^{-1} nm^4)	R$_0$ (nm)
CdSe/6CdS/2ZnS QDs	17.0	2.02	6.29

Acceptor	Molar Extinction Coefficient (M^{-1} cm^{-1})
Cy5	250,000

Table A3. Synthetic DNA oligos for AIY binding.

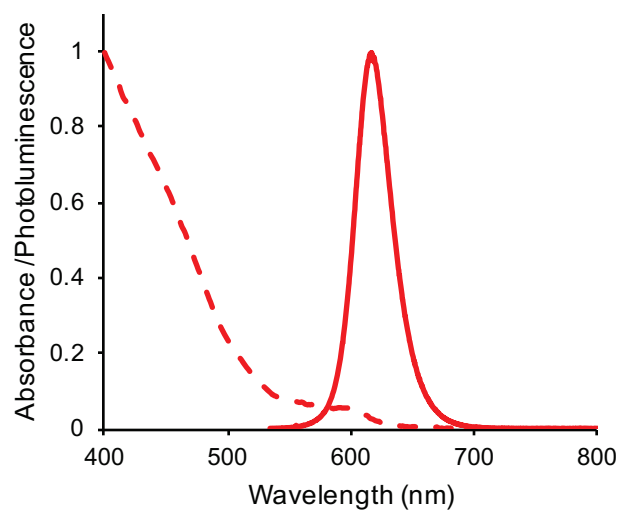| Name	Sequence [a]
AIY_DNA (forward)	5'-GTCA **TCCCTATCATTGATAGAGA** TACTG-3'
AIY_DNA' (reverse)	3'-**C**AGT **AGGGATAGTAACTATCTCT** ATGA**C**-5'
Scrambled (forward)	5'-TCGT GAAACCGAGCGAGGGACAC GCACA-3'
Scrambled (reverse)	3'-**A**GCA CTTTGGCTCGCTCCCTGTG CGTG**T**-5'

Figure A1. Absorbance (dashed line) and emission (solid line) spectra of QD2 used in AIY sensor.

BIBLIOGRAPHY

1. "Evaluation of Certain Mycotoxins in Food. Fifty-Sixth Report of the Joint FAO/WHO Expert Committee on Food Additives." *World Health Organization Technical Report Series*, vol. 906, 2002.

2. Arugula, Mary A, and Aleksandr Simonian. "Novel Trends in Affinity Biosensors: Current Challenges and Perspectives." *Measurement Science and Technology*, vol. 25, no. 3, 2014, p. 032001, doi:10.1088/0957-0233/25/3/032001.

3. Bermejo, Clara, et al. "Optical Sensors for Measuring Dynamic Changes of Cytosolic Metabolite Levels in Yeast." *Nature Protocols*, vol. 6, no. 11, 2011, pp. 1806–1817, doi:10.1038/nprot.2011.391.

4. Bolintineanu, Dan S., et al. "Investigation of Changes in Tetracycline Repressor Binding upon Mutations in the Tetracycline Operator." *Journal of Chemical & Engineering Data*, vol. 59, no. 10, 2014, pp. 3167–3176, doi:10.1021/je500225x.

5. Borisov, Sergey M., and Otto S. Wolfbeis. "Optical Biosensors." *Chemical Reviews*, vol. 108, no. 2, 2008, pp. 423–461, doi:10.1021/cr068105t.

6. Boyle, John. "Lehninger Principles of Biochemistry (4th Ed.): Nelson, D., and Cox, M." *Biochemistry and Molecular Biology Education*, vol. 33, no. 1, 2005, pp. 74–75, doi:10.1002/bmb.2005.494033010419.

7. Breitling, Rainer, and Eriko Takano. "Synthetic Biology Advances for Pharmaceutical Production." *Current Opinion in Biotechnology*, vol. 35, 2015, pp. 46–51, doi:10.1016/j.copbio.2015.02.004.

8. Chern, Margaret, et al. "Sensing with Photoluminescent Semiconductor Quantum Dots." *Methods and Applications in Fluorescence*, vol. 7, no. 1, 2019, p. 012005, doi:10.1088/2050-6120/aaf6f8.

9. Chern, Margaret, et al. "Shell Thickness Effects on Quantum Dot Brightness and Energy Transfer." *Nanoscale*, vol. 9, no. 42, 2017, pp. 16446–16458, doi:10.1039/c7nr04296e.

10. Chou, Kenny, and Allison Dennis. "Förster Resonance Energy Transfer between Quantum Dot Donors and Quantum Dot Acceptors." *Sensors*, vol. 15, no. 6, 2015, pp. 13288–13325, doi:10.3390/s150613288.

11. Clapp, Aaron R., et al. "Capping of CdSe–ZnS Quantum Dots with DHLA and Subsequent Conjugation with Proteins." *Nature Protocols*, vol. 1, no. 3, 2006, pp. 1258–1266, doi:10.1038/nprot.2006.184

12. Cuperus, Josh T., et al. "A TetO Toolkit to Alter Expression of Genes in Saccharomyces Cerevisiae." *ACS Synthetic Biology*, vol. 4, no. 7, 2015, pp. 842–852, doi:10.1021/sb500363y.

13. D'Mello, J.P.F.. Food Safety : Contaminants and Toxins, CABI, 2003. ProQuest Ebook Central, https://ebookcentral.proquest.com/lib/bu/detail.action?docID=295055.

14. Damborsky, P., et al. "Optical Biosensors." *Essays In Biochemistry*, vol. 60, no. 1, 2016, pp. 91–100, doi:10.1042/ebc20150010.

15. Dennis, Allison M., and Gang Bao. "Quantum Dot−Fluorescent Protein Pairs as Novel Fluorescence Resonance Energy Transfer Probes." *Nano Letters*, vol. 8, no. 5, 2008, pp. 1439–1445, doi:10.1021/nl080358+.

16. Dennis, Allison M., et al. "Surface Ligand Effects on Metal-Affinity Coordination to Quantum Dots: Implications for Nanoprobe Self-Assembly." *Bioconjugate Chemistry*, vol. 21, no. 7, 2010, pp. 1160–1170, doi:10.1021/bc900500m.

17. Fan, Xudong, et al. "Sensitive Optical Biosensors for Unlabeled Targets: A Review." *Analytica Chimica Acta*, vol. 620, no. 1-2, 2008, pp. 8–26, doi:10.1016/j.aca.2008.05.022.

18. Fechner, Peter, et al. "Size Does Matter! Label-Free Detection of Small Molecule–Protein Interaction." *Analytical and Bioanalytical Chemistry*, vol. 406, no. 17, 2014, pp. 4033–4051, doi:10.1007/s00216-014-7834-4.

19. Fodey, Terry, et al. "Developments in the Production of Biological and Synthetic Binders for Immunoassay and Sensor-Based Detection of Small Molecules." *TrAC: Trends in Analytical Chemistry*, vol. 30, no. 2, 2011, pp. 254–269, doi:10.1016/j.trac.2010.10.011.

20. Gao, Yuan, and Xiaogang Peng. "Photogenerated Excitons in Plain Core CdSe Nanocrystals with Unity Radiative Decay in Single Channel: The Effects of Surface and Ligands." *Journal of the American Chemical Society*, vol. 137, no. 12, 2015, pp. 4230–4235, doi:10.1021/jacs.5b01314.

21. Ghosh, Yagnaseni, et al. "New Insights into the Complexities of Shell Growth and the Strong Influence of Particle Volume in Nonblinking 'Giant' Core/Shell Nanocrystal Quantum Dots." *Journal of the American Chemical Society*, vol. 134, no. 23, 2012, pp. 9634–9643, doi:10.1021/ja212032q.

22. González-Peñas, E, et al. "Determination of Ochratoxin A in Wine Using Liquid-Phase Microextraction Combined with Liquid Chromatography with Fluorescence Detection." *Journal of Chromatography A*, vol. 1025, no. 2, 2004, pp. 163–168, doi:10.1016/j.chroma.2003.10.113.

23. Heyduk, Ewa, et al. "Molecular Beacons for Detecting DNA Binding Proteins: Mechanism of Action." *Analytical Biochemistry*, vol. 316, no. 1, 2003, pp. 1–10, doi:10.1016/s0003-2697(03)00004-6.

24. Heyduk, Tomasz, and Ewa Heyduk. "Molecular Beacons for Detecting DNA Binding Proteins." *Nature Biotechnology*, vol. 20, no. 2, 2002, pp. 171–176, doi:10.1038/nbt0202-171.

25. Ho, Cheng Hsun, and Wolf B. Frommer. "Fluorescent Sensors for Activity and Regulation of the Nitrate Transceptor CHL1/NRT1.1 and Oligopeptide Transporters." 2014. bioRχiv: doi:10.1101/002741.

26. Jawaid, Waqass, et al. "Development and Validation of a Novel Lateral Flow Immunoassay (LFIA) for the Rapid Screening of Paralytic Shellfish Toxins (PSTs) from Shellfish Extracts." *Analytical Chemistry*, vol. 87, no. 10, 2015, pp. 5324–5332, doi:10.1021/acs.analchem.5b00608.

27. Kamionka, A. "Two Mutations in the Tetracycline Repressor Change the Inducer Anhydrotetracycline to a Corepressor." *Nucleic Acids Research*, vol. 32, no. 2, 2004, pp. 842–847, doi:10.1093/nar/gkh200.

28. Kaper, Thijs, et al. "Nanosensor Detection of an Immunoregulatory Tryptophan Influx/Kynurenine Efflux Cycle." *PLoS Biology*, vol. 5, no. 10, 2007, doi:10.1371/journal.pbio.0050257.

29. Khansili, Nishtha, et al. "Label-Free Optical Biosensors for Food and Biological Sensor Applications." *Sensors and Actuators B: Chemical*, vol. 265, 2018, pp. 35–49, doi:10.1016/j.snb.2018.03.004.

30. Kiessling, K. H., et al. "Metabolism of Aflatoxin, Ochratoxin, Zearalenone, and Three Trichothecenes by Intact Rumen Fluid, Rumen Protozoa, and Rumen Bacteria." *Applied and Environmental Microbiology*, vol. 47, no. 5, May 1984, pp. 1070–1073.

31. Kim, Eun-Kyung, et al. "Liquid Chromatographic Determination of Fumonisins B1, B2, and B3 in Corn Silage." *Journal of Agricultural and Food Chemistry*, vol. 52, no. 2, 2004, pp. 196–200, doi:10.1021/jf034934t.

32. Lakowicz, Joseph R. *Principles of Fluorescence Spectroscopy*. Springer, 2006.

33. Li, Shanshan, et al. "A Platform for the Development of Novel Biosensors by Configuring Allosteric Transcription Factor Recognition with Amplified Luminescent Proximity Homogeneous Assays." *Chemical Communications*, vol. 53, no. 1, 2017, pp. 99–102, doi:10.1039/c6cc07244e.

34. Ligler, Frances S. "Perspective on Optical Biosensors and Integrated Sensor Systems." *Analytical Chemistry*, vol. 81, no. 2, 2009, pp. 519–526, doi:10.1021/ac8016289.

35. Mahr, Regina, and Julia Frunzke. "Transcription Factor-Based Biosensors in Biotechnology: Current State and Future Prospects." *Applied Microbiology and Biotechnology*, vol. 100, no. 1, 2015, pp. 79–90, doi:10.1007/s00253-015-7090-3.

36. Martín, Alejandro San, et al. "Imaging Mitochondrial Flux in Single Cells with a FRET Sensor for Pyruvate." *PLoS ONE*, vol. 9, no. 1, 2014, doi:10.1371/journal.pone.0085780.

37. Medintz, Igor L., et al. "Quantum Dot Bioconjugates for Imaging, Labelling and Sensing." *Nature Materials*, vol. 4, no. 6, 2005, pp. 435–446, doi:10.1038/nmat1390.

38. Mohsin, Mohd., and Altaf Ahmad. "Genetically-Encoded Nanosensor for Quantitative Monitoring of Methionine in Bacterial and Yeast Cells." *Biosensors and Bioelectronics*, vol. 59, 2014, pp. 358–364, doi:10.1016/j.bios.2014.03.066.

39. Nie, Jingjing, et al. "Electrochemical Detection of Tobramycin Based on Enzymes-Assisted Dual Signal Amplification by Using a Novel Truncated Aptamer with High Affinity." *Biosensors and Bioelectronics*, vol. 122, 2018, pp. 254–262, doi:10.1016/j.bios.2018.09.072.

40. Peltomaa, Riikka, et al. "Optical Biosensors for Label-Free Detection of Small Molecules." *Sensors*, vol. 18, no. 12, 2018, p. 4126, doi:10.3390/s18124126.

41. Peroza, Estevão A., et al. "A Genetically Encoded Förster Resonance Energy Transfer Sensor for Monitoring in Vivo Trehalose-6-Phosphate Dynamics." *Analytical Biochemistry*, vol. 474, 2015, pp. 1–7, doi:10.1016/j.ab.2014.12.019.

42. Susumu, Kimihiro, et al. "Multifunctional Compact Zwitterionic Ligands for Preparing Robust Biocompatible Semiconductor Quantum Dots and Gold Nanoparticles." *Journal of the American Chemical Society*, vol. 133, no. 24, 2011, pp. 9480–9496, doi:10.1021/ja201919s.

43. Turner, Anthony P. F., et al. *Biosensors: Fundamentals and Applications*. Oxford University Press, 1989.

44. Verma, Neelam, and Atul Bhardwaj. "Biosensor Technology for Pesticides—A Review." *Applied Biochemistry and Biotechnology*, vol. 175, no. 6, 2015, pp. 3093–3119, doi:10.1007/s12010-015-1489-2.

45. Vinkenborg, Jan L, et al. "Genetically Encoded FRET Sensors to Monitor Intracellular Zn2+ Homeostasis." *Nature Methods*, vol. 6, no. 10, 2009, pp. 737–740, doi:10.1038/nmeth.1368.

46. Visconti, Angelo, and Michelangelo Pascale. "Determination of Zearalenone in Corn by Means of Immunoaffinity Clean-up and High-Performance Liquid Chromatography with Fluorescence Detection." *Journal of Chromatography A*, vol. 815, no. 1, 1998, pp. 133–140, doi:10.1016/s0021-9673(98)00296-9.

47. Wang, Xiang-Hong, and Shuo Wang. "Sensors and Biosensors for the Determination of Small Molecule Biological Toxins." *Sensors*, vol. 8, no. 9, 2008, pp. 6045–6054, doi:10.3390/s8096045.

48. Yu, Xuezhi, et al. "Universal Simultaneous Multiplex ELISA of Small Molecules in Milk Based on Dual Luciferases." *Analytica Chimica Acta*, vol. 1001, 2018, pp. 125–133, doi:10.1016/j.aca.2017.11.038.

49. Zhang, Dongdong, et al. "Simultaneous Detection of Forbidden Chemical Residues in Milk Using Dual-Label Time-Resolved Reverse Competitive Chemiluminescent Immunoassay Based on Amine Group Functionalized Surface." *PLoS ONE*, vol. 9, no. 10, 2014, doi:10.1371/journal.pone.0109509.

50. Zhang, Jie, et al. "Development of Biosensors and Their Application in Metabolic Engineering." *Current Opinion in Chemical Biology*, vol. 28, 2015, pp. 1–8, doi:10.1016/j.cbpa.2015.05.013.

CURRICULUM VITAE